Ultra-high-strength polyethylene filaments by solution spinning/drawing

PAUL SMITH, PIET J. LEMSTRA
Central Laboratory, DSM, Geleen, The Netherlands

This paper deals with ultra-high-strength monofilaments of linear polyethylene that are produced by solution spinning and subsequent hot drawing at 120° C. The influence of the draw ratio on the mechanical and thermal properties of the fibres was investigated. Some salient features of a polyethylene filament with a draw ratio of 31.7 are: tensile strength at break = 3.0 GPa, Young's modulus = 90 GPa and DSC-melting point at a scan speed of 10° C min^{-1} = 145.5° C. The modulus was found to depend linearly on the draw ratio. The tensile strength tended, by contrast, to approach an upper limit at high draw ratios. Additional morphological and X-ray studies revealed an extremely good orientation of the macromolecules in the fibre direction of the highly drawn polyethylene monofilaments.

1. Introduction

Since the chain character of polymer molecules was recognized some 50 years ago many attempts have been made to exploit the intrinsically anisotropic properties of these materials. For this purpose extension and alignment of macromolecules have been studied throughout the years. Nowadays a variety of methods are known to produce orientation in polymers, such as cold, hot and zone drawing, direct and hydrostatic extrusion and radial compression of polymer rods [1–9]. In these methods the polymer is processed below its end melting point. Chain extension and alignment have also been achieved in polymer melts and solutions by the action of flow fields (see e.g. [10–16]).

Peterlin [17] pointed out that orientation of macromolecules by processing in the solid state will be much more effective than in the liquid state. This is due to the drastically higher viscosity of the solid, because of which the relaxation phenomena counteracting the molecular orientation are negligible if compared with those in the liquid. The relatively rapid relaxation of macromolecules in the liquid state, however, can be inhibited by fixation of the oriented chains in a crystalline lattice. This was demonstrated in studies on hydrodynamically induced crystallization of polyethylene from supercooled solutions that were subjected to flow [10–14]. In this process still some relaxation of the polymer molecules might have occurred, which can be judged from the properties of the crystals produced.

More recently Zwijnenburg and Pennings reported on a technique referred to as surface growth, that is performed in a Couette-type apparatus [18]. In this mode of solution crystallization a longitudinally growing polyethylene crystal is in close contact with the rotor onto which a layer of polymer molecules is thought to be adsorbed [18, 19]. The macromolecules that are connected with the growing crystal and the rotor surface experience a continuous strain preventing the chains to return to a coiled conformation. In this manner effective extension of the molecules occurs, that is known to enhance the nucleation and growth of polymer crystals [20]. Indeed, longitudinal growth rates were measured that were substantially higher than the "free-growth" rates in Couette flow [19]. The properties of these surface grown filaments were superior to those of the fibres obtained by hydrodynamically induced crystallization [21], longitudinal crystallization in Poiseuille and Couette flow [22], and also if compared with the characteristics of polyethylene structures generated by any solid-state process. For example, the Young's modulus and

the tensile strength of surface grown polyethylene filaments may amount up to 100 GPa and 3 GPa, respectively [22]. The modulus of solid-state extruded and drawn material may be as high as 70 GPa, but the tensile strength is usually found below 1 GPa [23, 24]. The major disadvantage of the surface growth process of Zwijnenburg and Pennings is that until now the production rate of the longitudinal crystals is far below commercially interesting speeds [19].

In this paper we present an alternative method to produce ultra-high-strength polyethylene filaments with a Young's modulus of 90 GPa and a tensile strength of 3 GPa. This method is based on a simple solution-spinning and hot-drawing technique that can be performed continuously and at high speeds. A preliminary account of this work was given earlier [26].

2. Experimental

The high molecular weight polyethylene Hostalen GUR ($\bar{M}_w = 1.5 \times 10^6$ and $\bar{M}_n = 2 \times 10^5$) was used in this study. The solvent was decalin, a mixture of cis- and transdecahydronaphtalene, from J. T. Baker Chemicals. Solutions were prepared by dissolving 2% w/w of the polymer in decalin at 150° C. To prevent degradation of the polyethylene, the dissolution was carried out under nitrogen and the solutions were stabilized with 0.5% w/w antioxidant (di-t-butyl-p-cresol).

Polyethylene filaments were spun using the experimental set up that is shown schematically in Fig. 1. The highly viscous polymer solution

was pumped at 130° C through capillaries with diameters ranging from 0.5 to 1.0 mm and a length of 3.0 mm. The as-spun liquid filament was quenched in cold water to form a gel fibre. This continuous gel filament was subsequently drawn in a hot-air oven at 120° C and at a strain rate of about 1 sec⁻¹, to yield a solvent free, highly oriented, polyethylene structure.

Stress—strain curves of these monofilaments were recorded at room temperature using an Instron tensile-tester (model 1195). The initial sample length was 15 cm. It was found that variations in the speed of testing in the range 1 to 10 cm min⁻¹ did not affect the stress—strain behaviour. A crosshead speed of 10 cm min⁻¹ was maintained throughout this study.

Differential scanning calorimetric (DSC) measurements were carried out on unconstrained fibre specimens with a length of about 15 cm. The calorimeter was manufactured by Perkin Elmer (DSC-II). The melting temperatures quoted in this paper invariably refer to the peak temperatures in the thermograms.

The polyethylene filaments were examined in the optical and scanning electron microscope.

Wide-angle and small-angle X-ray fibre patterns were obtained employing a flat-film camera. Ni-filtered CuKα-radiation was used.

3. Results

The method to produce high-strength and high-modulus polyethylene fibres described in the present paper essentially comprises two steps
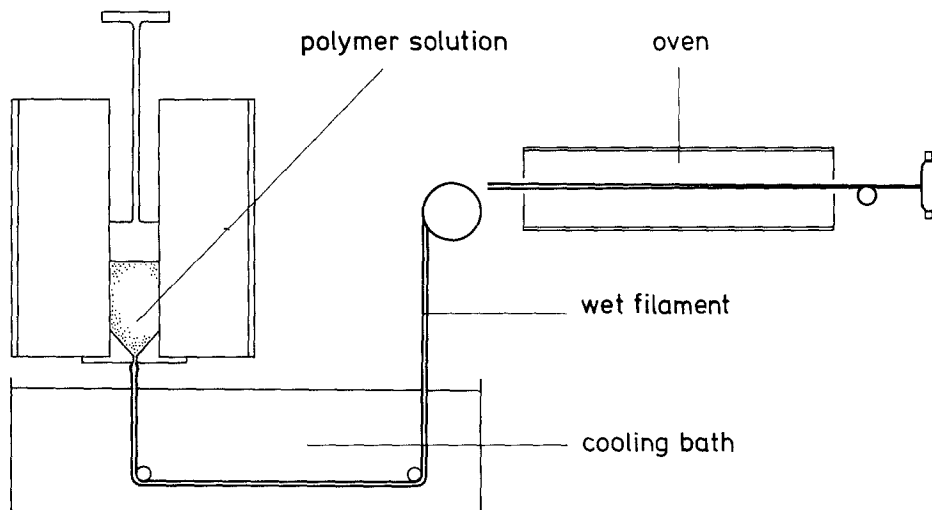
Figure 1 Schematic representation of the solution spinning/drawing process.
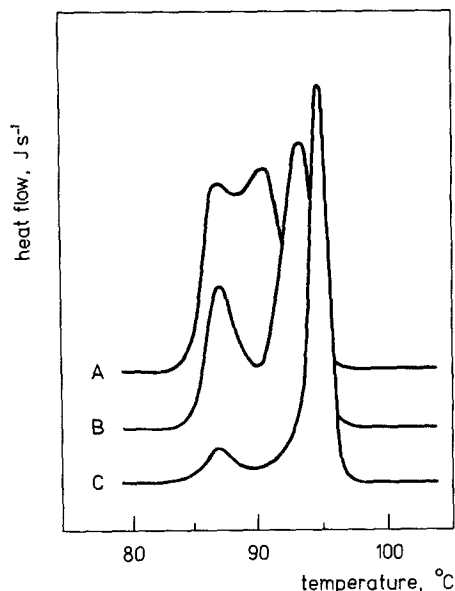
Figure 2 DSC-heating thermograms of polyethylene/ decalin gel. Scan speeds: A 40° C min^{-1}; B 20° C min^{-1}; C 5° C min^{-1}.

(solution spinning and hot drawing) which will be dealt with consecutively.

3.1. Solution spinning

In the first stage of the process the highly viscous polyethylene solution was pumped through a capillary to form a liquid filament that was subsequently quenched in a cooling bath. A gel fibre with a slightly opaque appearance was thus generated, containing almost all of the solvent.

Unexpectedly, this polyethylene gel filament appeared to be fairly strong and elastic, considering the minor amount of polymer it contained.

The load-to-break of a gel filament with a diameter of 0.7 mm was 49 g, which corresponds to a tensile strength of 1×10^4 Pa. The Young's modulus was 9×10^4 Pa, and the elongation at break amounted to 350% at room temperature.

In order to elucidate some structural features of the gel fibres thermal analysis, optical microscopy and wide-angle X-ray scattering (WAXS) studies were performed.

Fig. 2 presents DSC-heating thermograms of the polyethylene gels that were recorded at different scan speeds. At a heating rate of 40° C min^{-1} (curve A) the thermogram was composed of two endotherms, at 87° C and 92° C. Upon reduction of the scan speed the peak at the lower temperature decreased in area. The high-temperature endotherm, by contrast, increased in area and shifted towards higher temperatures at lower scan speeds. These observations are known to be a typical result of recrystallization phenomena during heating polymeric crystals [27]. Hence, it was rather problematic to measure the heat of dissolution of the polyethylene structure accurately. We nevertheless estimated its value to be 80 J g^{-1}, which points to a low polymer crystallinity.

Fig. 3 displays a photomicrograph of the polyethylene/decalin gel fibre as it was viewed in the polarizing microscope with crossed Nicols. Evidently, an unoriented structure with little bi-refringence is seen in this figure.

A WAXS-pattern of the gel filament is shown in Fig. 4. Also from this figure it was inferred that no persistent orientation was generated during the solution spinning and quenching step. The diffraction pattern displays one broad halo and
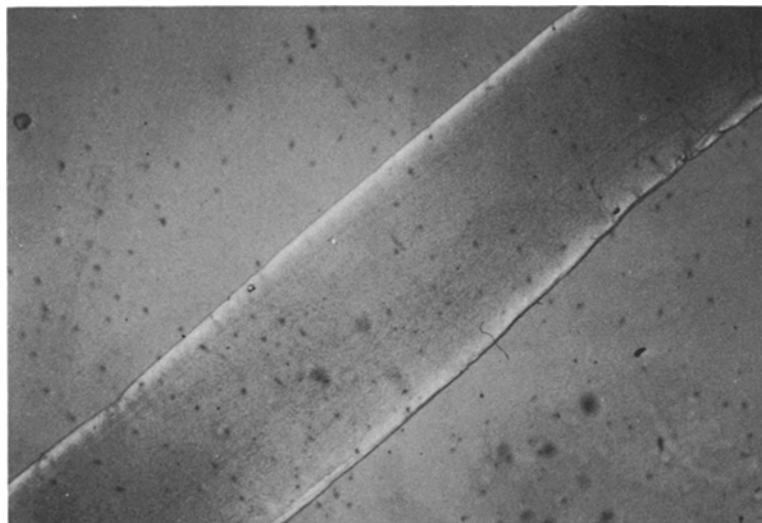
Figure 3 Optical micrograph of undrawn wet polyethylene/decalin gel. Crossed polarizers; magnification 28X.

507
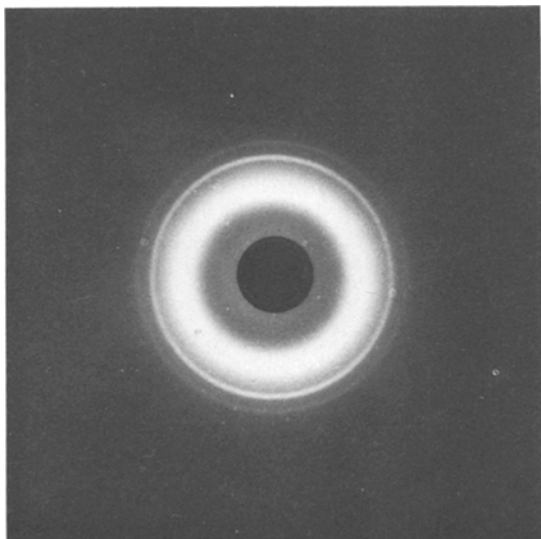
Figure 4 WAXS-pattern of polyethylene/decalin gel.

some weak, but rather sharp reflections. The latter were identified as the (1 1 0) and (2 0 0) reflections of the orthorhombic crystal structure of polyethylene at an angle of 21.5° and 24.2°, respectively. The diffuse halo at a lower angle is due to the solvent.

Based on the morphological, DSC and WAXS data we arrived at the conclusion that upon quenching the liquid filament a gel fibre was formed, the structure of which is thought to be a macroscopic network of polymer molecules with crystallites acting as physical cross-links. These crystals may very well have a fibrillar nature, since they were generated from a flowing solution of high molecular weight polyethylene [10].

3.2. Hot drawing
In the second stage of the solution spinning/ drawing process the polyethylene gel fibre was subjected to hot drawing. It was found that high draw ratios readily could be achieved at temperatures in the range from 90 to 135° C, i.e. roughly between the "dissolution temperature" of the gel and the melting point of the pure polymer. At lower temperatures frequently fracture occurred upon drawing. A drawing temperature of 120° C appeared to be convenient and was maintained throughout the study. On the influence of the drawing temperature will be reported in a forthcoming paper. The strain rate employed was about $1 \, sec^{-1}$. After this hot drawing no detectable

amount of solvent was left in the highly drawn polyethylene filaments.

3.3. Mechanical properties
In Fig. 5 typical stress–strain curves are presented of solution-spun/drawn polyethylene filaments. The draw ratios indicated refer to the reduction in the cross-sectional area of the drawn fibres in comparison with dried undrawn filaments. This area was calculated from the mass per unit length of the fibres, and the density.

Fig. 5 shows that the drawing process drastically improved the mechanical properties of the filaments, which, in fact, is well known for polymeric materials. The Young's modulus, tensile strength and strain at break that were calculated from these stress–strain curves are listed in Table I.

The Young's modulus is plotted against the draw ratio in Fig. 6. As is illustrated in this figure we found a linear relationship between modulus and draw ratio. Similar unique, even if not necessarily linear relations between modulus and draw ratio were previously observed by other authors in drawing [24, 25], solid-state extrusion [23] and radial compression of polyethylene rods [9].

The tensile strength of the solution-spun/drawn polyethylene filaments is plotted as a function of the draw ratio in Fig. 7. Also here a simple relation was found, similar to trends previously reported [23]. Like the modulus, the tensile strength initially
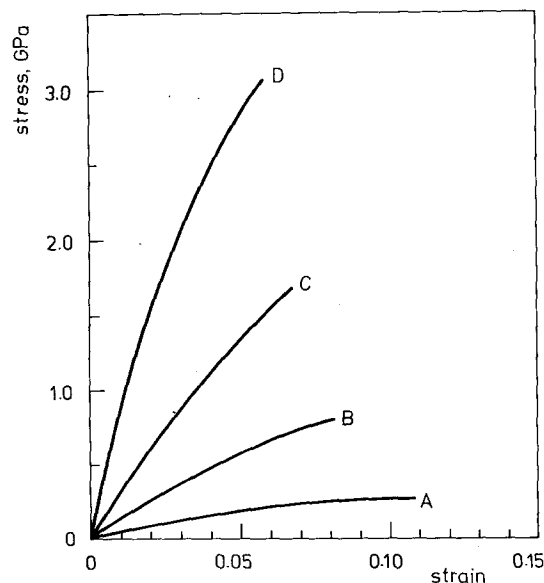
Figure 5 Stress–strain curves of solution-spun/drawn polyethylene fibres. Draw ratios: A 2.8; B 8.4; C 15.7; D 31.7.

Draw ratio	Modulus (GPa)	Tensile strength (GPa)	Strain at break
1.0	2.4	0.06	0.722
2.8	5.4	0.27	0.108
7.3	17.0	0.73	0.076
8.4	17.6	0.81	0.083
8.6	25.1	1.17	0.090
9.4	24.1	1.38	0.072
9.8	27.5	1.39	0.070
10.3	28.3	1.52	0.074
10.4	28.1	1.27	0.065
11.3	23.9	1.32	0.071
12.1	37.5	1.65	0.074
13.1	40.9	1.72	0.063
13.9	32.6	1.45	0.065
15.7	41.2	1.80	0.068
25.5	68.3	2.87	0.059
31.7	90.2	3.04	0.060

increases linearly with the draw ratio. At high draw ratios, however, the strength tends to approach an upper limit.

It is of interest to note that in the present spinning/drawing technique both the modulus and the tensile strength increase more rapidly with increasing draw ratio than in drawing melt-spun material, or in materials prepared by extrusion and radial compression [9, 23, 24]. It is even more striking that the tensile strength increases as much with increasing draw ratio as the Young's modulus,

which can be judged from Table I. This observation is unlike results obtained in the solid-state deformation processes quoted before, where the tensile strength increases much more slowly with the draw ratio than the modulus. Consequently, the tensile strength's of the solution-spun/drawn polyethylene filaments exceed by far the reported values of other drawn and extruded samples. In fact, the tensile strength of 3.0 GPa of a 31.7 times drawn fibre ranks among the highest data of polyethylene fibres obtained by the surface growth technique of Zwijnenburg and Pennings [22].

The strain at break of the filaments rapidly drops with increasing draw ratio to reach a constant value of 0.06 for ratios exceeding 15, as is illustrated in Fig. 8.

3.4. Melting behaviour

This section deals in brief with the thermal properties of the polyethylene fibres, which were studied by differential scanning calorimetry. It should be mentioned that a standard heating rate of $10°C$ min^{-1} was adopted in all experiments. It is well known that the highly oriented polymer structures we are currently dealing with may exhibit pronounced superheating effects [28]. Hence the melting temperatures presented in this paper should be compared with those measured under similar conditions.
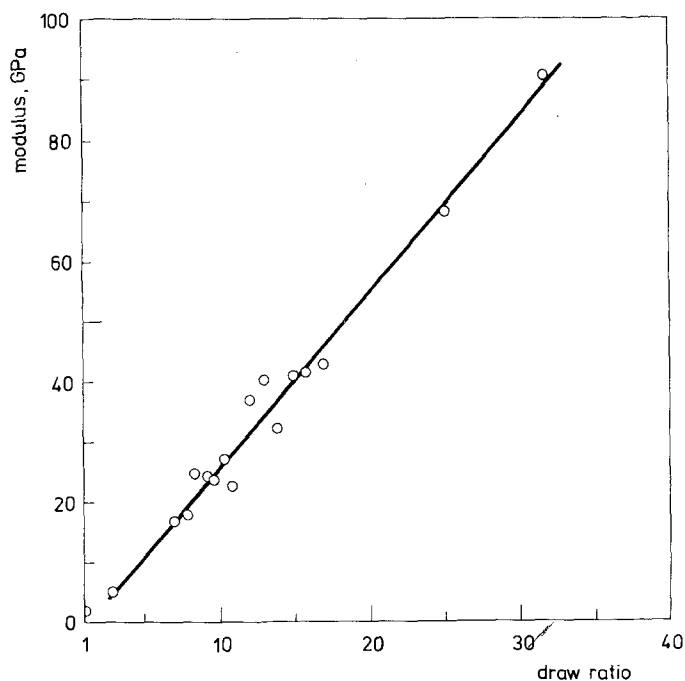
Figure 6 Young's modulus–drawn ratio relationship of polyethylene filaments.
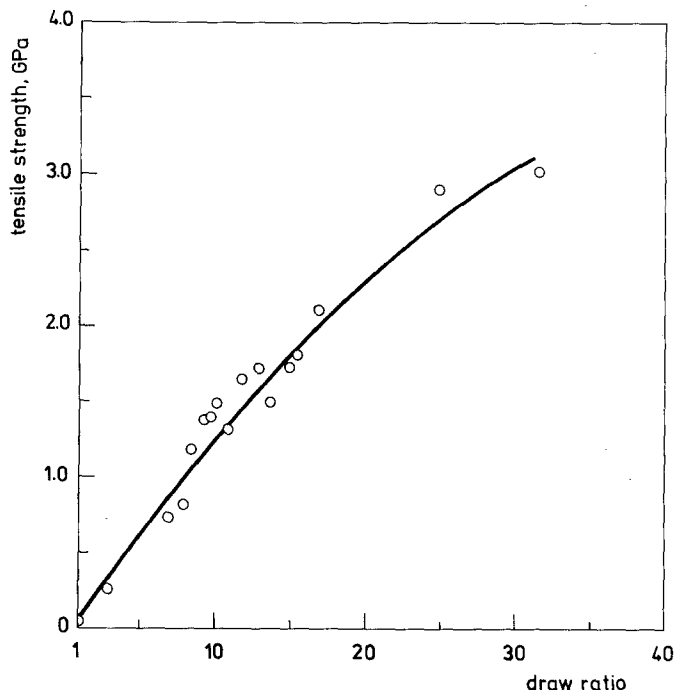
Figure 7 Tensile strength versus draw ratio of polyethylene filaments.

In Fig. 9 DSC-thermograms are presented of the dried undrawn fibre and of fibres with draw ratios of 15.7 and 31.7. Similar to the mechanical properties, the thermal characteristics were found to depend strongly on the draw ratio, as was observed previously by other authors (e.g. [29]). The undrawn monofilament had a peak melting temperature of 133.0° C and the 15.7 times drawn fibre 141.0° C. Curve C of the filament with a draw ratio of 31.7 exhibits one pronounced maximum at 145.5° C and a second small peak at 152.0° C. This second endotherm may be due to a solid–solid transformation from the orthorhombic crystalline phase to the hexagonal one, as was found in melting longitudinal polyethylene crystals by Pennings and Zwijnenburg [30].

The peak melting temperatures of various polyethylene fibres are presented in Fig. 10. The melting point rapidly increases with draw ratio reaching asymptotically a value of 145.5° C at a draw ratio of 31.7. This value is substantially higher than the melting temperatures of drawn or extruded polyethylene samples [29, 31]. It agrees very well with the highest melting point of surface
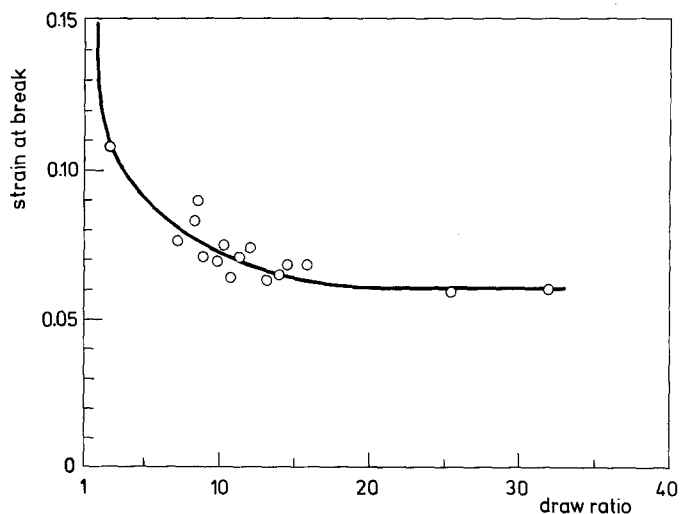
Figure 8 Dependence of the strain at break on the draw ratio.

510
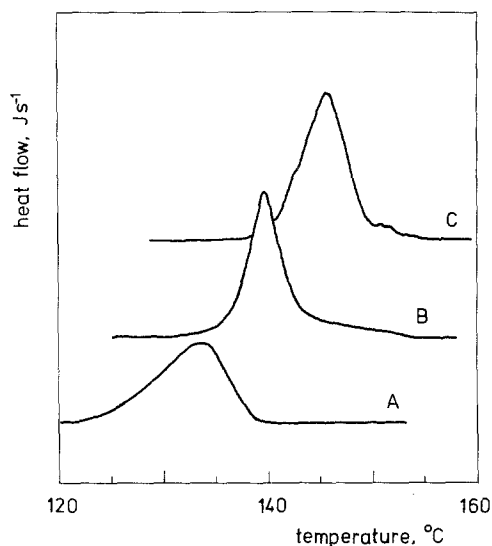
Figure 9 DSC-heating thermograms of solution-spun/drawn polyethylene fibres. Scan speed $10°\,C\,min^{-1}$. Draw ratios: A 1; B 15.7; C 31.7.

grown longitudinal crystals, measured under identical conditions [30].

The heat of fusion of the filaments showed a similar dependence on the draw ratio as the melting temperature. The value of the dried undrawn sample was $163\,J\,g^{-1}$. The heat of fusion of the drawn fibres rapidly increased with the draw ratio, reaching a value of $260\,J\,g^{-1}$ at a ratio of 31.7. This corresponds to an increase in crystallinity from 56 to 90% if based on a value of $293\,J\,g^{-1}$ for fully crystalline polyethylene.

3.5. Structure
Some morphological and structural features of the solution-spun/drawn polyethylene filaments revealed by optical and scanning electron microscopy
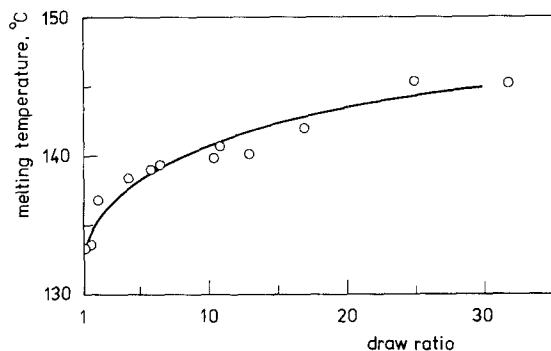
Figure 10 DSC-(peak)melting temperatures versus draw ratio of polyethylene monofilaments.

and X-ray scattering will be described in this section.

Fig. 11 displays optical micrographs of dried undrawn (a) and 25.5 times drawn (b, c) fibres as viewed between crossed polarizers. The undrawn filament consisted of crystalline entities with no preferential orientation. The drawn fibre appeared, by contrast, to be uniformly oriented and highly bi-refringent (Fig. 11b). At higher magnifications (Fig. 11c) well-oriented striations were discerned in the filaments. The cross-sectional shape of the fibres was frequently found to be rectangular. For instance, the specimen shown in Figs. 11b and c had a thickness and a width of $8\,\mu m$ and $80\,\mu m$, respectively. The cause for this rectangular shape may be found in the fact that the wet gel fibre was wound up on a bobbin prior to drawing, which might have resulted in some lateral deformation.

The striations in the highly drawn filaments were seen in greater detail in the scanning electron microscope. The SEM photograph in Fig. 12 shows a polyethylene filament with a draw ratio of 31.7. The diameter of this fibre is $20\,\mu m$. This micrograph reveals that the surface of the filament is rather uniform and smooth, and has a fibrillar nature.

Information about the molecular arrangement in the drawn polyethylene filaments was obtained by wide-angle X-ray scattering. Fig. 13 shows WAXS-patterns of fibres with draw ratios of 1.5 (a), 15.7 (b) and 31.7 (c). The diffraction patterns are characterized by the typical $(1\,1\,0)$ and $(2\,0\,0)$ reflections of the orthorhombic polyethylene unit cell. The 1.5 times drawn fibre shows a slight c- and a-axis orientation. The latter type of orientation was reported previously for polyethylene specimens with low draw ratios [32]. From Figs. 13b and c it was inferred that increasing draw ratio leads, expectedly, to a drastic increase in orientation of the polymer molecules in the fibre direction.

The highly drawn fibres did not display a discrete reflection in the small-angle region of the X-ray scattering pattern, which points to a rather continuous crystalline nature of these filaments.

4. Discussion
In this paper we presented a simple route to produce high-strength and high-modulus polyethylene filaments. There seems to be a close resemblance between the solution-spinning/drawing process and

511
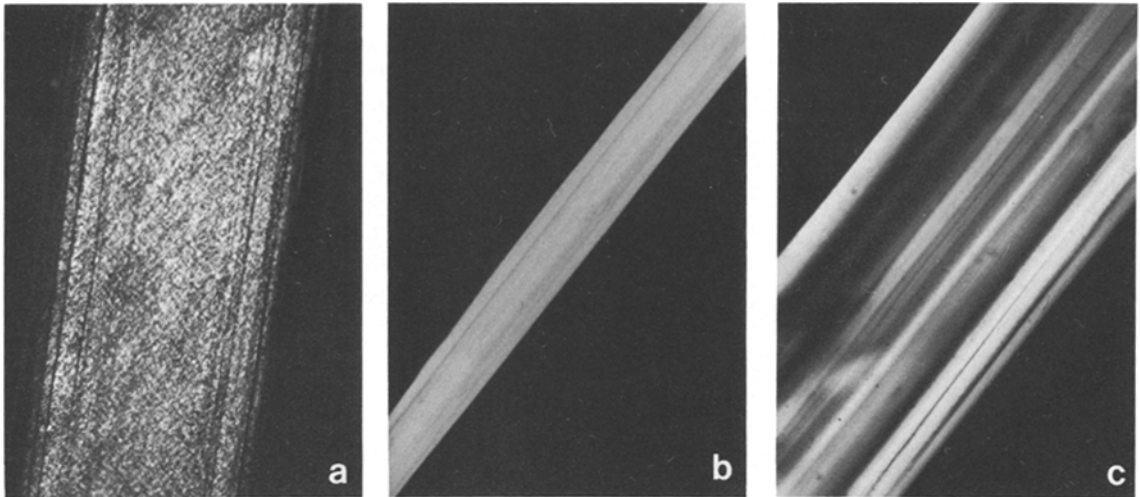
Figure 11 Optical micrographs of polyethylene fibres. Crossed Nicols. a draw ratio 1, magnification 96×; b draw ratio 25.5, magnification 120×; c draw ratio 25.5, magnification 480×.

the well-known drawing and extrusion techniques. This is indicated by the draw ratio/modulus, strength or melting temperature relationships observed in the three methods. It should be noted, however, that the effectiveness of the present drawing process, the tensile strength and, to a lesser extent, the modulus and melting point of the fibres produced are superior in comparison with the other two techniques. The cause for this

difference is found both in the molecular weight of the polymer used, and in a drastically increased effective drawability of high molecular weight polyethylene that is spun or cast from dilute solutions, related to melt-processed material [33]. These topics will be dealt with extensively in future papers.

The properties of the solution-spun/drawn fibres and the crystals obtained by the surface growth
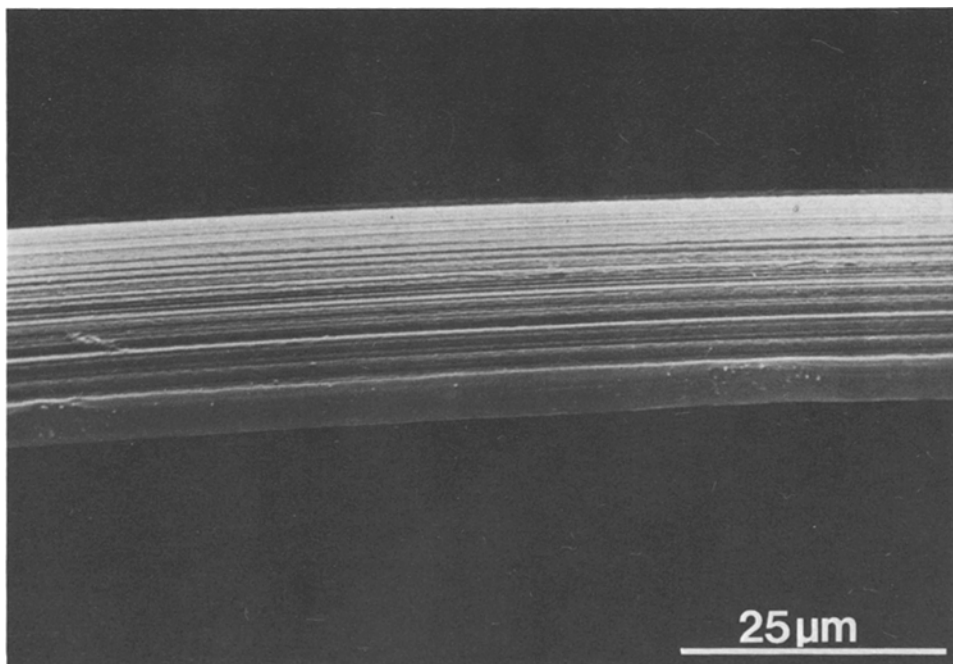
Figure 12 Scanning electron micrograph of a 31.7 times drawn polyethylene fibre.

512
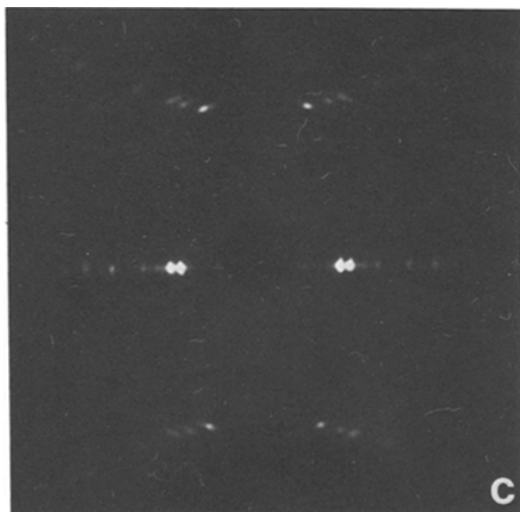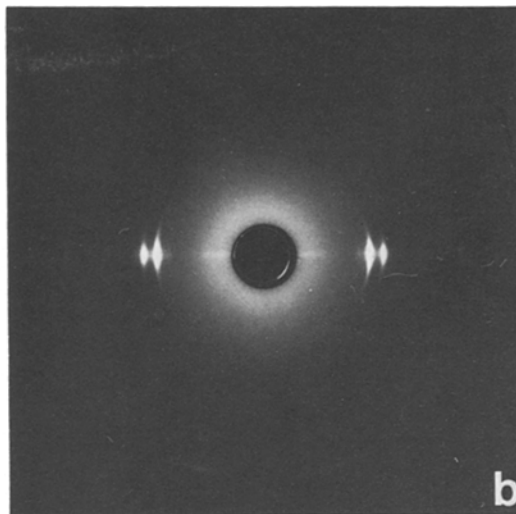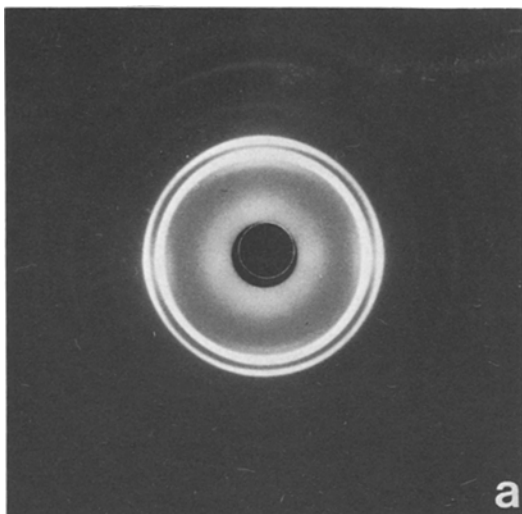
Figure 13 WAXS-patterns of drawn polyethylene filaments. Draw ratios: a 1.5; b 15.7; c 31.7. Fibre axis vertical.

mations by pulling alongside the rotor surface, or simply by hot drawing, to yield a highly oriented structure.

Acknowledgement

References

1. A. PETERLIN and G. MEINEL, *J. Polymer Sci B* **3** (1965) 783.
2. K. YAMADA, M. KAMAZAWA and M. TAKAYANAGI, *Polymer Preprints Amer. Chem. Soc.* (1979) 780.
3. M. TAKAYANAGI, K. IMADA and T. KAJIYAMA, *J. Polymer Sci. C* **15** (1966) 263.
4. J. H. SOUTHERN and R. S. PORTER, *J. Appl. Polymer Sci.* **14** (1970) 2305.
5. P. PREDECKI and W. O. STATTON, *J. Polymer Sci. B* **10** (1972) 87.
6. A. G. GIBSON, I. M. WARD, B. N. COLE and B. PARSONS, *J. Mater. Sci.* **9** (1974) 1193.
7. G. CAPACCIO and I. M. WARD, *Polymer* **15** (1974) 233.
8. E. S. CLARK and L. S. SCOTT, *Polymer Eng. Sci.* **14** (1974) 682.
9. P. D. GRISWOLD, R. S. PORTER, C. R. DESPER and R. J. FARRIS, *ibid.* **18** (1978) 537.
10. A. J. PENNINGS, J. M. A. A. VAN DER MARK and H. C. BOOIJ, *Kolloid Z.- Z. Polymere* **236** (1970) 99.
11. A. ZWIJNENBURG and A. J. PENNINGS, *Colloid & Polymer Sci.* **253** (1975) 452.
12. F. C. FRANK, A. KELLER and M. R. MACKLEY,

method show striking similarities, which prompts a comparison of these two seemingly different processes. At this stage, however, this appears to be rather premature in view of the scarcity of the available information. Nevertheless, recent observations by Barham *et al.* [34] concerning gel formation in dilute solutions of high molecular weight polyethylene and its relation to the so-called surface growth technique point to a basically identical mechanism of fibre formation. This mechanism involves the generation of a physical network of the polymer. In the surface growth process this gel is formed around the rotor of the Couette-apparatus, and in the present method the macromolecular network is formed in the solution-spinning/quenching stage. Subsequently the polymer gel is subjected to very large defor-

Polymer **12** (1971) 467.

13. M. R. MACKLEY and A. KELLER, *Phil. Trans. Roy. Soc. (London)* **A278** (1975) 29.
14. A. J. McHUGH and J. M. SCHULTZ, *Kolloid Z.- Z. Polymere* **251** (1973) 193.
15. A. KELLER, *J. Polymer Sci.* **15** (1955) 31.
16. H. D. KEITH, F. J. PADDEN and R. G. VADIMSKY, *J. Appl. Phys.* **37** (1966) 4027.
17. A. PETERLIN, *Polymer Eng. Sci.* **14** (1974) 627.
18. A. ZWIJNENBURG and A. J. PENNINGS, *Colloid & Polymer Sci.* **254** (1976) 868.
19. A. J. PENNINGS, *J. Polymer Sci. Polymer Symp.* **59** (1977) 55.
20. A. J. McHUGH, *J. Appl. Polymer Sci.* **19** (1975) 125.
21. A. J. PENNINGS, C. J. H. SCHOUTETEN and A. M. KIEL, *J. Polyer Sci. C.* **38** (1972) 167.
22. A. ZWIJNENBURG and A. J. PENNINGS, *J. Polymer Sci. Polymer Lett.* **14** (1976) 339.
23. S. KOJIMA and R. S. PORTER, *J. Polymer Sci. Polymer Phys. Ed.* **16** (1978) 1729.
24. G. CAPACCIO and I. M. WARD, *Polymer* **16** (1975) 239.
25. P. J. BARHAM and A. KELLER, *J. Mater. Sci.* **11** (1976) 27.
26. P. SMITH, P. J. LEMSTRA, B. KALB and A. J. PENNINGS, *Polymer Bull.* **1** (1979) 733.
27. B. WUNDERLICH, "Macromolecular Physics", Vol. 2 (Academic Press, New York, 1976). p. 390.
28. B. WUNDERLICH and G. CZORNYJ, *Macromolecules* **10** (1977) 906.
29. J. CLEMENTS, G. CAPACCIO and I. M. WARD, *J. Polymer Sci. Polymer Phys. Ed.* **17** (1979) 693.
30. A. J. PENNINGS and A. ZWIJNENBURG, *J. Polymer Sci. Polymer Phys. Ed.* **17** (1979) 1011.
31. S. KOJIMA, C. R. DESPER and R. S. PORTER, *ibid.* **16** (1978) 1721.
32. J. T. JUDGE and R. S. STEIN, *J. Appl. Phys.* **32** (1961) 2357.
33. P. SMITH and P. J. LEMSTRA, *Die Makromol. Chem.* (in press).
34. P. J. BARHAM, M. J. HILL, C. G. CANNON and A. KELLER, *Polymer Lett.* (submitted).